Investigating inducible short-chain alcohol dehydrogenases/reductases clarifies rice oryzalexin biosynthesis

Naoki Kitaoka[1], **Yisheng Wu**[2], **Jiachen Zi**[3], and **Reuben J. Peters**[*]

Roy J. Carver Department of Biochemistry, Biophysics, and Molecular Biology, Iowa State University, Ames, IA 50011, U.S.A

Summary

Rice (*Oryza sativa*) produces a variety of labdane-related diterpenoids as phytoalexins and allelochemicals. The production of these important natural products has been partially elucidated. However, the oxidases responsible for production of the keto groups found in many of these diterpenoids have largely remained unknown. Only one short-chain alcohol dehydrogenase/reductases (SDRs), which has been proposed to catalyze the last step in such a pathway, has been characterized to-date. While rice contains >220 SDRs, only the transcription of five has been shown to be induced by the fungal cell wall elicitor chitin. This includes the momilactone A synthase (OsMAS/SDR110C-MS1), with the other four all falling in the same SDR110C family, further suggesting roles in diterpenoid biosynthesis. Here biochemical characterization with simplified substrate analogs was first used to indicate potential functions, which were then supported by further analyses with key biosynthetic intermediates. Kinetic studies were then employed to further clarify these roles. Surprisingly, OsSDR110C-MS2 more efficiently catalyzes the final oxidation to produce momilactone A that was previously assigned to OsMAS/SDR110C-MS1, and we speculate that this latter SDR may have an alternative function instead. On the other hand, two of these SDRs clearly appear to act in oryzalexin biosynthesis, with OsSDR110C-MI3 readily oxidizing the 3α-hydroxyl of oryzalexin D, while OsSDR110C-MS3 can also oxidize the accompanying 7β-hydroxyl. Together, these SDRs then serve to produce oryzalexins A – C from oryzalexin D, essentially completing elucidation of the biosynthesis of this family of rice phytoalexins.

Keywords

diterpenoids; oxidases; phytoalexins; allelochemicals; biosynthesis

Introduction

Upon exposure to microbial pathogens plants produce an arsenal of antibiotic natural products, known as phytoalexins (Hammerschmidt 1999), which are considered to be an

[*]Corresponding author: rjpeters@iastate.edu.
[1]Current address: Department of Biomolecular Sciences, Graduate School of Life Sciences, Tohoku University, Sendai 980-8577, Japan
[2]Current address: Conagen Inc., Bedford, MA 01730, U.S.A.
[3]Current address: Biotechnological Institute of Chinese Materia Medica, College of Pharmacy, Jinan University, Guangzhou, Guangdong 510632, China

important part of the defense response (Bednarek and Osbourn 2009). Thus, the production of these metabolites is a subject of significant interest, as these compounds and/or the genes controlling their biosynthesis might serve as markers for molecular breeding, particularly in important crop plants, such as rice (*Oryza sativa*). One particularly interesting aspect of such plant natural products biosynthesis has been the observation of gene clusters containing unrelated genes encoding biosynthetic enzymes from a common metabolic pathway in certain cases (Nutzmann and Osbourn 2014).

Rice has served as a model cereal crop plant, including for investigation of phytoalexins, which appear to be almost all terpenoids (Schmelz *et al.* 2014). In particular, labdane-related diterpenoids whose biosynthesis is related to that of the gibberellin phytohormones in the characteristic use of a copalyl diphosphate synthase (CPS) to initiate their production from the general diterpenoid precursor (*E,E,E*)-geranylgeranyl diphosphate (Zi *et al.* 2014). These natural products have been suggested to serve as antibiotics against the fungal blast pathogen *Magneportha oryzae* [i.e., the momilactones, oryzalexins and phytocassanes (Peters 2006)] and bacterial leaf blight pathogen *Xanthomonas oryzae* [i.e., the oryzalides, oryzadiones and related compounds (Toyomasu 2008)], as well as allelochemicals that inhibit the growth of other plants [i.e., momilactone B (Kato-Noguchi and Peters 2013)].

The rice genome contains two biosynthetic gene clusters associated with labdane-related diterpenoid biosynthesis, one on chromosome 4 that appears to be dedicated to the production of momilactones (Shimura *et al.* 2007, Wilderman *et al.* 2004), while the other on chromosome 7 has been associated with the production of phytocassanes (Prisic *et al.* 2004, Swaminathan *et al.* 2009), although there is evidence that this cluster has a more general role in such biosynthesis – e.g., production of the oryzalexins and oryzalides as well (Wang *et al.* 2012a, Wu *et al.* 2011, Wu *et al.* 2013). In both cases, there is a gene encoding a CPS and at least one for a kaurene synthase-like (KSL) cyclase specific for the stereoisomer of CPP produced by the co-clustered CPS, along with several encoding cytochrome P450 (CYP) mono-oxygenases that will act on the resulting multicyclic diterpene olefins (e.g., Figure 1). Notably, the chromosome 4 cluster also contains a gene encoding a short-chain alcohol dehydrogenase/reductase (SDR), which has been suggested to catalyze the last step in momilactone A biosynthesis, oxidation of a 3β-hydroxyl to the characteristic keto group (Atawong *et al.* 2002), leading to its designation as the rice momilactone A synthase, OsMAS (Shimura, et al. 2007).

A number of other rice labdane-related diterpenoid phytoalexins also contain keto groups. While the CYPs that catalyze the initial addition of oxygen to form the relevant hydroxyl group have been identified in many cases, the enzyme catalyzing subsequent oxidation to a carbonyl has remained unknown. For example, CYP701A8 and CYP76M8 consecutively oxygenate *ent*-sandaracopimaradiene at C3α and then C7β, respectively, forming the di-hydroxy oryzalexin D (Wu, et al. 2013), further oxidation of which at C3 and/or C7 forms oryzalexins A – C (Peters 2006). Similarly, CYP76M7 can introduce a C11α hydroxyl group into *ent*-cassadiene, with the subsequently formed C11-keto found in all the phytocassanes (Swaminathan, et al. 2009), while CYP701A8 can introduce a C3α-hydroxyl, with either this or the derived 3-keto group found in all phytocassanes (Wang *et al.* 2012b),

and CYP71Z7 can introduce a C2α-hydroxyl, which also can be further oxidized to a keto – e.g., as in phytocassane D (Wu, et al. 2011).

While there are over 220 SDRs in rice (Moummou *et al.* 2012), it has already been shown that transcription of the genes encoding the relevant upstream enzymes for labdane-related diterpenoids are inducible (Schmelz, et al. 2014). A particularly broad view was provided by microarray based analysis of the transcriptional response of rice cell culture to induction with the fungal cell wall elicitor chitin (Okada *et al.* 2007). Notably, this study found significant accumulation of mRNA for five SDRs, including OsMAS. Here biochemical analysis of these SDRs was carried out and used to suggest their roles in rice labdane-related diterpenoid phytoalexin biosynthesis, leading most particularly to clarification of the production of oryzalexins.

Results

The inducible rice SDRs

The SDRs form one of the largest enzymatic super-families and are highly diverse. Hence, the SDRs have been divided into phylogenetically distinct broad classes and more specific families to assist functional annotation (Persson *et al.* 2009). All five of the chitin-inducible SDRs contain the TGxxxGxG coenzyme binding and YxxxK catalytic motifs that place them in the classical SDR class (Kavanagh *et al.* 2008), as well as a specific Asp indicating a preference for NAD^+ over $NADP^+$ (Kallberg *et al.* 2002)(Figure S1). More specifically, these all fall within the vascular plant specific SDR110C family, members of which generally oxidize terpenoid or phenolic compounds. Even more particularly, these inducible OsSDR110C family members are divided between two clades therein (Figure 2), one defined by OsMAS and that is termed here the momilactone synthase (MS) clade, and another simply annotated monocot I and termed here the MI clade (Moummou, et al. 2012). According to this nomenclature, OsMAS can be termed OsSDR110C-MS1 (referred to hereafter as MS1), while the other clearly inducible clade member is OsSDR110C-MS3 (MS3). Similarly, those from the MI clade are largely found in a tandem array of 13 such genes on chromosome 7, and the chitin inducible members of this are OsSDR110C-MI2 (MI2), OsSDR110C-MI3 (MI3) and OsSDR110C-MI4 (MI4). Full-length mRNA corresponding to all five of these SDRs have been reported from a previous large-scale cDNA sequence project and were obtained from this source (Kikuchi *et al.* 2003).

In addition to *OsMAS*, the momilactone biosynthetic gene cluster contains an adjacent and closely related SDR (OsSDR110C-MS2; hereafter MS2), which appears to have arisen by tandem gene duplication and shares >94% sequence identity with MS1 (Miyamoto *et al.* 2016). While the transcript of this gene was not reported to accumulate in response to chitin, it does not appear to have been separately represented on the microarray. Accordingly, it seemed plausible that this SDR might play a role in momilactone biosynthesis and/or other labdane-related diterpenoid phytoalexin biosynthesis. Thus, MS2 was also investigated here. Due to difficulties in cloning this, presumably in part as a result of the exact identity at both the 5' and 3' ends of the coding regions of this and MS1, a synthetic gene was obtained instead.

Initial biochemical analyses with simplified substrate analogs

The full length SDRs were recombinantly expressed as N-terminal 6xHis-tagged proteins in *Escherichia coli* strain C41 and purified via affinity chromatography. Recombinant protein was obtained for all these SDRs except MI4, which was not expressed well and, thus, not further investigated here. Based on previous work, a variety of mono-hydroxylated labdane-related diterpenes are readily available (Kitaoka *et al.* 2015, Swaminathan, et al. 2009, Wang, et al. 2012a, Wang *et al.* 2011, Wang, et al. 2012b, Wu, et al. 2011, Wu, et al. 2013). Hypothesizing that activity against these various hydroxyl groups might highlight potential roles for these SDRs in phytoalexin biosynthesis, these diterpene alcohols were tested as potential substrates (Figure 3). For example, 11α-hydroxy-*ent*-cassadiene provides the alcohol that presumably is oxidized as an early step in phytocassane biosynthesis (Figure 1), while 3β-hydroxy-*syn*-pimaradiene presents the relevant alcohol that is oxidized to form momilactone A (Figure 3). All assays also included 1 mM NAD$^+$ to provide this necessary enzymatic co-factor, with organic extracts analyzed by GC-MS to detect the presence of oxidized products (i.e., a new peak with an apparent molecular ion of $m/z = 286$, relative to the $m/z = 288$ observed with the mono-hydroxylated diterpene precursors).

While none of the SDRs reacted with 11α-hydroxy-*ent*-cassadiene, four of them reacted with 3β-hydroxy-*syn*-pimaradiene to varying degrees, with only MI2 unable to oxidize this (Table 1 and Figure S2). Surprisingly, MS1 was actually somewhat less active than not only MS2, but also MI3 with this latter substrate, which provides the relevant alcohol for the originally suggested reaction. Indeed, MS1 exhibited greater turnover with the alternative substrate 2α-hydroxy-*ent*-cassadiene, which was further oxidized by the other SDRs, with the exception of MI2 again (Table 1 and Figure S3). Similarly, these same four SDRs were able to oxidize both 3α-hydroxy-*ent*-cassadiene and 3α-hydroxy-*ent*-sandaracopimaradiene to varying degrees as well, although only MS3 was able to oxidize 7β-hydroxy-*ent*-sandaracopimaradiene (Table 1 and Figures S4 – S6). These initial results suggest that these SDRs are mostly likely to play roles in momilactone and/or oryzalexin biosynthesis, with any role in the production of phytocassanes occurring at later steps for which the relevant intermediates have not yet been identified and, thus, are not yet available.

SDRs in momilactone biosynthesis

The ability of multiple SDRs to catalyze oxidation of 3β-hydroxy-*syn*-pimaradiene suggested that the analogous step in momilactone A biosynthesis might be mediated by more than just MS1. This possibility was investigated by directly assaying these with 3β-hydroxy-*syn*-pimaradien-19,6β-olide, the penultimate intermediate in momilactone A biosynthesis (Atawong, et al. 2002), and originally reported MS1 substrate (Shimura, et al. 2007). Consistent with the results from assays with the simplified substrate analog 3β-hydroxy-*syn*-pimaradiene, not only MS1, but also MS2, MS3 and MI3 were able to produce momilactone A from 3β-hydroxy-*syn*-pimaradien-19,6β-olide (Figure 4, Table 1). Nevertheless, kinetic analysis demonstrated that MS1 and MS2 from the momilactone biosynthetic gene cluster exhibited significantly higher catalytic efficiency for this reaction than MS3 and MI3, for which kinetic constants could not be obtained due to poor substrate affinity (see Table 2). Somewhat surprisingly, MS2 exhibited much higher (>20-fold)

catalytic efficiency than MS1, with both higher affinity (i.e., lower K_M) and rate of catalysis (i.e., k_{cat}).

SDRs in oryzalexin biosynthesis

The ability of these SDRs to catalyze oxidation of the 3α and/or 7β hydroxylated derivatives of *ent*-sandaracopimaradiene suggested that these might play a role in oryzalexin biosynthesis. In particular, the oxidation of oryzalexin D to oryzalexins A – C, which was investigated by directly assaying these SDRs with oryzalexin D (Figure 5). Again consistent with the results from the simplified substrate analogs, the same four SDRs were found to oxidize oryzalexin D (Table 1). In each case a new product was observed in which the apparent molecular ion was $m/z = 302$, representing oxidation of a single hydroxyl of oryzalexin D ($m/z = 304$). In addition, MS3 yielded two additional products, another with an apparent molecular ion of $m/z = 302$, and one with an apparent molecular ion of $m/z = 300$, presumably representing oxidation of both hydroxyl groups (i.e., oryzalexin C).

Given that only MS3 was able to oxidize 7β-hydroxy-*ent*-sandaracopimaradiene, while all four SDRs can oxidize 3α-hydroxy-*ent*-sandaracopimaradiene, it seemed likely that the common SDR product was selectively oxidized at C3 (i.e., oryzalexin B). This was verified by scaling up the *in vitro* enzyme reaction to produce sufficient amounts for NMR analysis. Briefly, 0.5 mg of oryzalexin D was obtained by metabolic engineering of *E. coli*, as previously described (Wu, et al. 2013). This was converted to the common oxidized product with MS1. After extraction and purification, 0.2 mg of this compound was isolated. The resulting ^{1}H-NMR data matched that reported for oryzalexin B rather than oryzalexin A (Kono *et al.* 1985). Accordingly, the remaining MS3 product is then oryzalexin A, resulting from oxidation of the 7β-hydroxyl group, again consistent with the activity observed with the corresponding simplified substrate analog.

To further investigate the relevance of the observed activity to oryzalexin biosynthesis, kinetic analysis was carried out for all four SDR with oryzalexin D. Notably, MS3 and MI3 exhibited much higher catalytic efficiency (>100-fold) with this substrate than MS1 and MS2, the reverse of what is observed with the 3β-hydroxy-*syn*-pimaradien-19,6β-olide intermediate in momilactone biosynthesis (Table 2).

Discussion

The studies described here provide some insight into the roles played by the investigated inducible SDRs in rice labdane-related diterpenoid biosynthesis. While all four SDRs that exhibit activity will react with multiple labdane-related diterpenoids (Table 1), such promiscuity is not entirely unexpected (Wu *et al.* 2007). Moreover, their ability to react with the simplified substrate analogs employed here provided useful suggestions regarding potentially relevant biosynthetic activity, with subsequent kinetic analyses indicating distinct roles for these oxidases (Table 2).

Perhaps clearest are the results indicating that MS3 and MI3 catalyze oxidation of the 7β- and/or 3α-hydroxyl groups, respectively, in production of oryzalexins A – C (Figure 6). This is particularly indicated by the strong catalytic efficiency exhibited by these OsSDR110C

family members with oryzalexin D (Table 2), and their relatively weak activity with the corresponding mono-hydroxylated derivatives of *ent*-sandaracompimaradiene argues that oryzalexin D is the relevant precursor to oryzalexins A – C (i.e., rather than proceeding via oxidation and then secondary hydroxylation). Although it remains unclear if there is a preferential route to the fully/dually oxidized oryzalexin C (i.e., via oryzalexin A or B), given that both are observed, and the promiscuity exhibited by MS3, it seems likely that either route can be utilized in planta. Accordingly, these results essentially complete elucidation of the oryzalexin family of phytoalexins.

The location of *MS1* and *MS2* in the momilactone biosynthetic gene cluster imply a role for these in the production of momilactone A and/or B. Somewhat surprisingly, MS2 exhibits higher catalytic efficiency for oxidation of 3β-hydroxy-*syn*-pimaradien-19,6β-olide to momilactone A than MS1 (Table 2), which was previously suggested to carry out this reaction (Shimura, et al. 2007). Indeed, MS1 actually exhibits higher catalytic efficiency for oxidation of oryzalexin D to oryzalexin B, and both MS1 and MS2 actually seem to have higher affinity for oryzalexin D than 3β-hydroxy-*syn*-pimaradien-19,6β-olide (Table 2). Thus, while MS2 presumably is responsible for the final step in production of momilactone A, it will be of interest to further probe if MS1 has a different role in momilactone or other rice diterpenoid phytoalexin biosynthesis.

Finally, although it seems likely that oxidation of an 11α-hydroxyl group occurs early in phytocassane biosynthesis given the presence of an 11-keto group in all of these phytoalexins, the relevant SDR does not appear to be among those investigated here. On the other hand, the ability of the investigated SDRs to readily oxidize simplified substrate analogs suggests that these SDRs might be relevant to the oxidation of 2α- and 3α-hydroxyl groups that presumably represent latter steps in phytocassane biosynthesis. Nevertheless, it will be necessary to carry out further studies to identify the presumably early acting C11 oxidase. While all three members of the MS clade from rice have already been investigated here, of particular interest in these future studies will be the twelve as of yet uncharacterized members of the MI clade from the SDR110C family found in rice.

Material and methods

General

Unless otherwise noted, chemicals were purchased from Fisher Scientific (Loughborough, Leicestershire, UK), and molecular biology reagents from Invitrogen (Carlsbad, CA, USA). Gas chromatography (GC) was performed with a Varian (Palo Alto, CA) 3900 GC equipped with an HP-5MS column (Agilent, 0.25 μm, 0.25ID, 30 m) and 1.2 L mL/min He flow rate, with detection via a Saturn 2100 ion trap mass spectrometer (MS) in electron ionization mode (70 eV). Samples (1 μL) were injected in splitless mode with the injection port at 250 °C and oven at 50 °C, after holding for 3 min. at 50 °C the oven temperature was raised at 15 °C/min. to 300 °C, where it was held for an additional 3 min. MS data from 90 to 600 mass-to-charge ratio (*m/z*) was collected from 14 min. after injection until the end of the run. GC with flame ionization detection (GC-FID) was carried out with an Agilent 6890N GC also equipped with an HP-5MS column and using the same temperature program. High pressure liquid chromatography (HPLC) was carried out with an Agilent 1100 HPLC system

equipped with auto-sampler, fraction collector and diode-array detector, run in reversed phase at 0.5 mL/min with a ZORBAX Eclipse XDB-C8 column (150 x 4.6 mm, 5 μm), using deionized water (dH$_2$O) and acetonitrile (AcN). NMR spectra were recorded at 25 °C on a Bruker Avance 700 spectrometer (^{1}H 700 MHz; ^{13}C 174 MHz) equipped with a 5-mm HCN cryogenic probe for ^{1}H and ^{13}C, using standard experiments from the Bruker TopSpin v1.3 software. Compounds were dissolved in 0.5 mL deuterated chloroform (CDCl$_3$) and placed in microtubes (Shigemi; Allison Park, PA) for analysis, with chemical shifts referenced using the known chloroform (^{13}C 77.23, ^{1}H 7.24 ppm) signals offset from trimethyl-silane.

Substrate preparation

Oryzalexin D, 3α-hydroxy-*ent*-(sandaraco)pimara-8(14),15-diene, 7β-hydroxy-*ent*-sandaracopimaradiene, 2α-hydroxy-*ent*-cassa-12,15-diene, 3α-hydroxy-*ent*-cassadiene, 11α-hydroxy-*ent*-cassadiene, and 3β-hydroxy-*syn*-pimara-7,15-diene were produced using a bacterial metabolic engineering system and purified as previously described (Kitaoka, et al. 2015, Swaminathan, et al. 2009, Wang, et al. 2012a, Wang, et al. 2011, Wang, et al. 2012b, Wu, et al. 2011, Wu, et al. 2013). 3β-Hydroxy-*syn*-pimara-7,15-dien-19,6β-olide was prepared by reduction of momilactone A as previously described (Kato *et al.* 1977). Briefly, lithium aluminium hydride (0.5 mg) was added to anhydrous ether solution (1 mL) containing 0.5 mg momilactone A. After continuously stirring at room temperature for 10 minutes, water was slowly poured into the reaction mixture. This was then twice extracted with an equal volumne of ether, and the combined organic phase was dried over Na$_2$SO$_4$ and dried *in vacuo*. The residue was resuspended in 50% AcN/dH$_2$O, and purified by HPLC. After loading the sample, the column was washed for 2 min. with 50% (v/v) AcN/dH$_2$O, with a gradient from 2 – 25 min. raising the AcN to 100%, and the column washed from 25 – 35 min. with 100% AcN. Fractions containing 3β-hydroxy-*syn*-pimaradien-19,6β-olide were identified by GC-MS analysis, pooled and dried under N$_2$. Structural analysis was carried out using 1D ^{1}H, DQF-COSY, HSQC, HMBC and NOESY spectra acquired at 700 MHz and ^{13}C spectra acquired at 174 MHz. Correlations from the HMBC spectra were used to propose the majority of the structure, while connections between protonated carbons were obtained from DQF-COSY to complete the partial structure and assign proton chemical shifts. NOESY spectra provided Nuclear Overhauser Effect (NOE) cross-peak signal between the proton on C3 and that on C5 to assign the stereochemistry at C3. The ^{1}H-NMR spectrum (700 MHz, CDCl$_3$): δ 5.82 (1H, dd, *J* = 17.7, 11.7 Hz, H15), 5.64 (1H, d, *J* = 5.0 Hz, H5), 4.95 (1H, d, *J* = 17.7 Hz, H16*Z*), 4.90 (2H, m, H-6, H16*E*), 3.62 (1H, m, H3), 2.15 (1H, d, *J* = 11.7 Hz, H14b), 2.04 (1H, m, H2a), 1.99 (1H, dd, *J* = 11.7, 2.0 Hz, H15), 1.78 (1H, m H2b), 1.77 (1H, d, *J* = 3.9 Hz, H5), 1.64 (1H, m, H11b), 1.63 (1H, m, H9), 1.52 (1H, m, H12a), 1.52 (3H, s, H18), 1.50 (1H, m, H12b), 1.36 (1H, m, H1a), 1.31 (1H, m, H1b), 1.28 (1H, m, H11a), 1.04 (3H, s, H20), 0.84 (3H, s, H17). The ^{13}C-NMR spectrum (174 MHz, CDCl$_3$): 181.9 (C19), 149.6 (C8), 149.1 (C15), 114.4 (C7), 110.0 (C16), 74.6 (C6), 74.4 (C3), 51.3 (C9), 47.3 (C14), 46.9 (C5), 44.5 (C4), 40.1 (C13), 37.6 (C12), 33.1 (C10), 31.7 (C1), 29.4 (C2), 23.8 (C20), 22.9 (C18), 22.6 (C11), 21.9 (C17).

Recombinant construct and protein purification

OsMAS/SDR110C-MS1, *OsSDR110C-MS3*, *OsSDR110C-MI2*, *OsSDR110C-MI3*, and *OsSDR110C-MI4* were obtained from the KOME rice cDNA databank (GeneBank accessions AK103462, AK110700, AK107157, AK070585, and AK06856, respectively). After several attempts to clone *OsSDR110C-MS2* (GeneBank accession AK240900) were unsuccessful, resulting in only amplification of *MS1*, which has identical sequences at both the 5' and 3' ends of the coding region (corresponding to the primers used here), an alternative version was obtained by gene synthesis (GeneScript), with codon optimization for expression in *E. coli* (see supporting data for sequence). These were cloned into pENTR/SD/D-TOPO, and then transferred to pDEST17 by LR recombination before verification by complete gene sequencing. The resulting expression vectors were transformed into *E. coli* C41 OverExpress (Lucigen). The resulting recombinant bacteria were grown in 50 mL NZY medium at 37 °C overnight, and these cultures used to inoculate 1 L NYZ medium, and also shaken at 37 °C until their OD_{600} reached ~0.6–0.8. The culture was then induced with 1 mM isopropyl β-D-1-thiogalactopyranoside (IPTG), shaken at 16 °C for 16 hours. The bacteria were harvested by centrifugation and resuspended in 20 mL lysis buffer (50 mM Bis-Tris, 150 mM KCl, 20 mM Mg_2SO_4, 10% glycerol, 1 mM DTT, pH6.8). The cells were lysed by brief sonication and the soluble enzyme fraction was obtained by centrifugation (15,000 *g*, 25 min, 4 °C). The soluble enzyme fraction was incubated (rotating) with a slurry of Ni-NTA resin (2 mL) for 2 hours at 4 °C. The resin was washed by 20 mL wash buffer (50 mM Bis-Tris, 150 mM KCl, 20 mM imidazole, pH 6.8) and then eluted by 5 mL elution buffer (50 mM Bis-Tris, 150 mM KCl, 250 mM imidazole, pH 6.8). The imidazole was removed by dialysis, using 12–15 KDa cut-off membrane (Spectrum Chemical and Laboratory Products, Gardena, CA), twice against 1 L dialysis buffer (20 mM Tris-HCl, 150 mM KCl, 10% glycerol, pH 7.8). The resulting SDRs were utilized for enzymatic assays.

Enzymatic assays

Initial assays were conducted with 0.5 μM SDR, 50 μM substrate and 1 mM NAD^+ in 0.5 mL Tris-HCl buffer (100 mM Tris-HCl, pH 8.0) with 10% (v/v) glycerol. After incubating at 30 °C for 1 hour, the reaction mixture was extracted thrice with 0.5 mL *n*-hexanes. The organic extracts were combined, dried under N_2 gas and resuspended in 80 μL hexanes for analysis by GC-MS. Control assays were conducted without enzyme. Oxidation of the simplified substrate analogs was demonstrated by the reduction in *m/z* of the molecular ion from 288 to 286 in the mass spectra of the SDR and NAD^+ dependent product peaks. Oxidation of 3β-hydroxy-*syn*-pimara-7,15-dien-19,6β-olide was verified by comparison of the SDR and NAD^+ dependent product peak to a previously reported authentic sample of momilactone A (Xu *et al.* 2012).

Kinetic analysis was carried out using 10–40 nM recombinant SDR in 0.5 mL assays run for 5–10 min at 30 °C, as determined by preliminary analyses to lie within the linear response range. The oxygenated diterpene substrates were added in varying concentrations (10–300 μM). To stop the reaction, assay vials were placed on ice and the enzymatic products immediately extracted with *n*-hexanes as above, and quantified by analysis with GC-FID.

Verification of oryzalexin B

Oryzalexin D (0.5 mg) was oxidized by MS1 as described above (40 nM SDR and 50 μM substrate), with the assay run overnight at 30 °C. This was then extracted trice with an equal volumne of hexanes, and the pooled extract was dried under N_2 gas, and the residue redissolved in 50% AcN/dH_2O for HPLC purification. After loading the sample, the column was washed for 2 min. with 50% (v/v) AcN/dH_2O, with a gradient from 2 – 7 min. raising the AcN to 100%, and the column washed from 7 – 20 min. with 100% AcN. Fractions containing oryzalexin B were identified by GC-MS analysis, pooled and dried under N_2 gas. The structure was confirmed by comparison of the ^{1}H-NMR spectrum (700 MHz, CDCl$_3$) with that previously reported (Kono, et al. 1985): δ 5.70 (1H, dd, J = 17.5, 10.3 Hz), 5.51 (1H, br.s), 4.87 (1H, d, J = 17.5 Hz), 4.86 (1H, d, J = 10.3), 4.18 (1H, br.s), 2.56 (1H, td, J = 14.5, 6.0 Hz), 2.26 (1H, dt, J = 14.5, 3.7 Hz), 2.1 (1H, t, J = 7.5 Hz), 1.98 (1H, dd, J = 11.8, 4.2 Hz), 1.93 (1H, ddd, 13.3, 5.7, 3.3 Hz), 1.20 ~ 1.69 (7H), 1.03 (3H, s), 0.992 (3H, s), 0.987 (3H, s), 0.90 (3H, s).

Supplementary Material

Refer to Web version on PubMed Central for supplementary material.

Acknowledgments

References

Atawong A, Hasegawa M, Kodama O. Biosynthesis of rice phytoalexin: enzymatic conversion of 3β-hydroxy-9β-pimara-7,15-dien-19,6β-olide to momilactone A. Biosci Biotechnol Biochem. 2002; 66:566–570. [PubMed: 12005050]

Bednarek P, Osbourn A. Plant-microbe interactions: chemical diversity in plant defense. Science. 2009; 324:746–748. [PubMed: 19423814]

Hammerschmidt R. PHYTOALEXINS: What Have We Learned After 60 Years? Annual review of phytopathology. 1999; 37:285–306.

Kallberg Y, Oppermann U, Jornvall H, Persson B. Short-chain dehydrogenases/reductases (SDRs). European journal of biochemistry / FEBS. 2002; 269:4409–4417.

Kato T, Aizawa H, Tsunekawa M, Sasaki N, Kitahara Y, Takahashi N. Chemical transformations of the diterpene lactones momilactones A and B. J Chem Soc, Perkin Trans I. 1977:250–254.

Kato-Noguchi H, Peters RJ. The role of momilactones in rice allelopathy. J Chem Ecol. 2013; 39:175–185. [PubMed: 23385366]

Kavanagh KL, Jornvall H, Persson B, Oppermann U. Medium- and short-chain dehydrogenase/reductase gene and protein families : the SDR superfamily: functional and structural diversity within a family of metabolic and regulatory enzymes. Cellular and molecular life sciences : CMLS. 2008; 65:3895–3906. [PubMed: 19011750]

Kikuchi S, Satoh K, Nagata T, Kawagashira N, Doi K, Kishimoto N, Yazaki J, Ishikawa M, Yamada H, Ooka H, Hotta I, Kojima K, Namiki T, Ohneda E, Yahagi W, Suzuki K, Li CJ, Ohtsuki K, Shishiki T, Otomo Y, Murakami K, Iida Y, Sugano S, Fujimura T, Suzuki Y, Tsunoda Y, Kurosaki T, Kodama T, Masuda H, Kobayashi M, Xie Q, Lu M, Narikawa R, Sugiyama A, Mizuno K, Yokomizo S, Niikura J, Ikeda R, Ishibiki J, Kawamata M, Yoshimura A, Miura J, Kusumegi T, Oka M, Ryu R, Ueda M, Matsubara K, Kawai J, Carninci P, Adachi J, Aizawa K, Arakawa T, Fukuda S, Hara A, Hashidume W, Hayatsu N, Imotani K, Ishii Y, Itoh M, Kagawa I, Kondo S, Konno H, Miyazaki A, Osato N, Ota Y, Saito R, Sasaki D, Sato K, Shibata K, Shinagawa A, Shiraki T, Yoshino M,

Hayashizaki Y. Collection, mapping, and annotation of over 28,000 cDNA clones from *japonica* rice. Science. 2003; 301:376–379. [PubMed: 12869764]

Kitaoka N, Wu Y, Xu M, Peters RJ. Optimization of recombinant expression enables discovery of novel cytochrome P450 activity in rice diterpenoid biosynthesis. Appl Microbiol Biotechnol. 2015; 99:7549–7558. [PubMed: 25758958]

Kono Y, Takeuchi S, Kodama O, Sekido H, Akatsuka T. Novel phytoalexins (oryzalexins A, B and C) isolated from rice blast leaves infected with *Pyricularia oryzae* Part II: Structural studies of oryzalexins. Agric Biol Chem. 1985; 49:1695–1701.

Miyamoto K, Fujita M, Shenton MR, Akashi S, Sugawara C, Sakai A, Horie K, Hasegawa M, Kawaide H, Mitsuhashi W, Nojiri H, Yamane H, Kurata N, Okada K, Toyomasu T. Evolutionary trajectory of phytoalexin biosynthetic gene clusters in rice. Plant J. 2016

Moummou H, Kallberg Y, Tonfack LB, Persson B, van der Rest B. The plant short-chain dehydrogenase (SDR) superfamily: genome-wide inventory and diversification patterns. BMC Plant Biol. 2012; 12:219. [PubMed: 23167570]

Nutzmann HW, Osbourn A. Gene clustering in plant specialized metabolism. Curr Opin Biotechnol. 2014; 26:91–99. [PubMed: 24679264]

Okada A, Shimizu T, Okada K, Kuzuyama T, Koga J, Shibuya N, Nojiri H, Yamane H. Elicitor induced activation of the methylerythritol phosphate pathway towards phytoalexin biosynthesis in rice. Plant Mol Biol. 2007; 65:177–187. [PubMed: 17634747]

Persson B, Kallberg Y, Bray JE, Bruford E, Dellaporta SL, Favia AD, Duarte RG, Jornvall H, Kavanagh KL, Kedishvili N, Kisiela M, Maser E, Mindnich R, Orchard S, Penning TM, Thornton JM, Adamski J, Oppermann U. The SDR (short-chain dehydrogenase/reductase and related enzymes) nomenclature initiative. Chem Biol Interact. 2009; 178:94–98. [PubMed: 19027726]

Peters RJ. Uncovering the complex metabolic network underlying diterpenoid phytoalexin biosynthesis in rice and other cereal crop plants. Phytochemistry. 2006; 67:2307–2317. [PubMed: 16956633]

Prisic S, Xu M, Wilderman PR, Peters RJ. Rice contains two disparate *ent*-copalyl diphosphate synthases with distinct metabolic functions. Plant Physiol. 2004; 136:4228–4236. [PubMed: 15542489]

Schmelz EA, Huffaker A, Sims JW, Christensen SA, Lu X, Okada K, Peters RJ. Biosynthesis, elicitation and roles of monocot terpenoid phytoalexins. Plant J. 2014; 79:659–678. [PubMed: 24450747]

Shimura K, Okada A, Okada K, Jikumaru Y, Ko KW, Toyomasu T, Sassa T, Hasegawa M, Kodama O, Shibuya N, Koga J, Nojiri H, Yamane H. Identification of a biosynthetic gene cluster in rice for momilactones. J Biol Chem. 2007; 282:34013–34018. [PubMed: 17872948]

Swaminathan S, Morrone D, Wang Q, Fulton DB, Peters RJ. CYP76M7 is an *ent*-cassadiene C11α-hydroxylase defining a second multifunctional diterpenoid biosynthetic gene cluster in rice. Plant Cell. 2009; 21:3315–3325. [PubMed: 19825834]

Toyomasu T. Recent Advances Regarding Diterpene Cyclase Genes in Higher Plants and Fungi. Biosci Biotechnol Biochem. 2008; 72:1168–1175. [PubMed: 18460786]

Wang Q, Hillwig ML, Okada K, Yamazaki K, Wu Y, Swaminathan S, Yamane H, Peters RJ. Characterization of CYP76M5-8 indicates metabolic plasticity within a plant biosynthetic gene cluster. J Biol Chem. 2012a; 287:6159–6168. [PubMed: 22215681]

Wang Q, Hillwig ML, Peters RJ. CYP99A3: Functional identification of a diterpene oxidase from the momilactone biosynthetic gene cluster in rice. Plant J. 2011; 65:87–95. [PubMed: 21175892]

Wang Q, Hillwig ML, Wu Y, Peters RJ. CYP701A8: A rice *ent*-kaurene oxidase paralog diverted to more specialized diterpenoid metabolism. Plant Physiol. 2012b; 158:1418–1425. [PubMed: 22247270]

Wilderman PR, Xu M, Jin Y, Coates RM, Peters RJ. Identification of *syn*-pimara-7,15-diene synthase reveals functional clustering of terpene synthases involved in rice phytoalexin/allelochemical biosynthesis. Plant Physiol. 2004; 135:2098–2105. [PubMed: 15299118]

Wu X, Knapp S, Stamp A, Stammers DK, Jornvall H, Dellaporta SL, Oppermann U. Biochemical characterization of TASSELSEED 2, an essential plant short-chain dehydrogenase/reductase with broad spectrum activities. FEBS J. 2007; 274:1172–1182. [PubMed: 17298439]

Wu Y, Hillwig ML, Wang Q, Peters RJ. Parsing a multifunctional biosynthetic gene cluster from rice: Biochemical characterization of CYP71Z6 & 7. FEBS Lett. 2011; 585:3446–3451. [PubMed: 21985968]

Wu Y, Wang Q, Hillwig ML, Peters RJ. Picking sides: Distinct roles for CYP76M6 and -8 in rice oryzalexin biosynthesis. Biochem J. 2013; 454:209–216. [PubMed: 23795884]

Xu M, Galhano R, Wiemann P, Bueno E, Tiernan M, Wu W, Chung IM, Gershenzon J, Tudzynski B, Sesma A, Peters RJ. Genetic evidence for natural product-mediated plant-plant allelopathy in rice (*Oryza sativa*). New Phytol. 2012; 193:570–575. [PubMed: 22150231]

Zi J, Mafu S, Peters RJ. To Gibberellins and Beyond! Surveying the Evolution of (Di)Terpenoid Metabolism. Annu Rev Plant Biol. 2014; 65:259–286. [PubMed: 24471837]
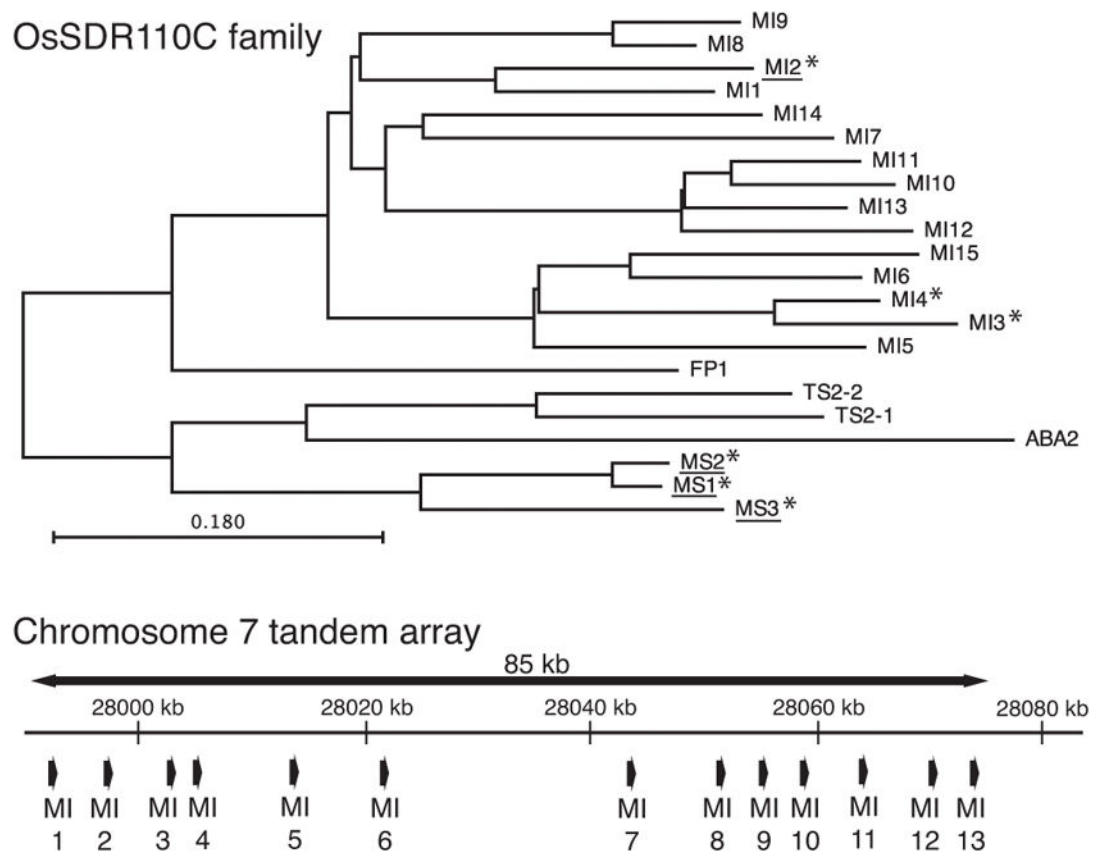
Figure 1.
Biosynthetic gene clusters and prospective pathways for phytocassanes A – F and momilactones A & B.

Figure 2.
The rice SDR110C family. Phylogenetic analysis of the two main clades (*, inducible transcript accumulation; underlined, biochemical characterization). Almost all of the members of the monocot I (MI) clade are found in a tandem gene array.
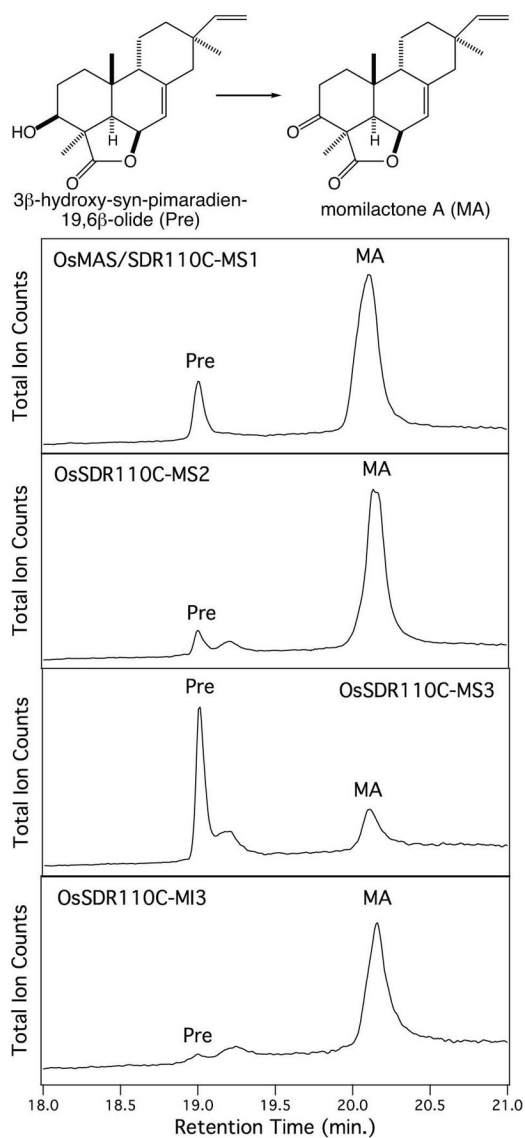
Figure 3.
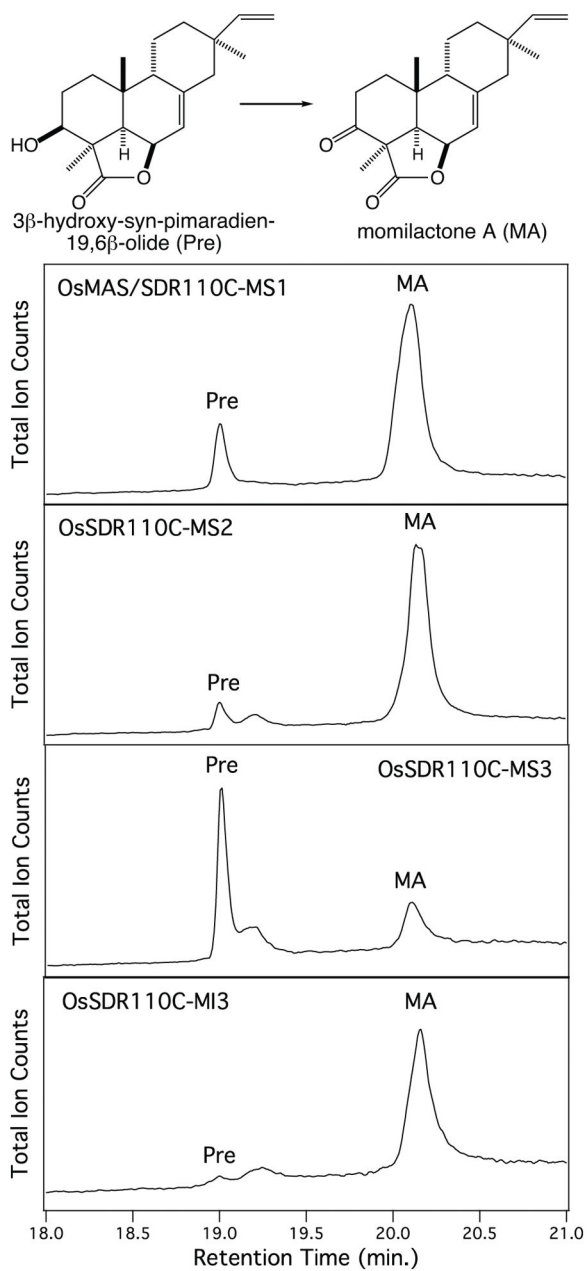Simplified substrate analogs of oxo group containing rice diterpenoids.

Figure 4.
SDR catalyzed oxidation of the precursor 3β-hydroxy-*syn*-pimaradien-19,6β-olide (Pre) to momilactone A (MA), as indicated by GC-MS chromatograms.
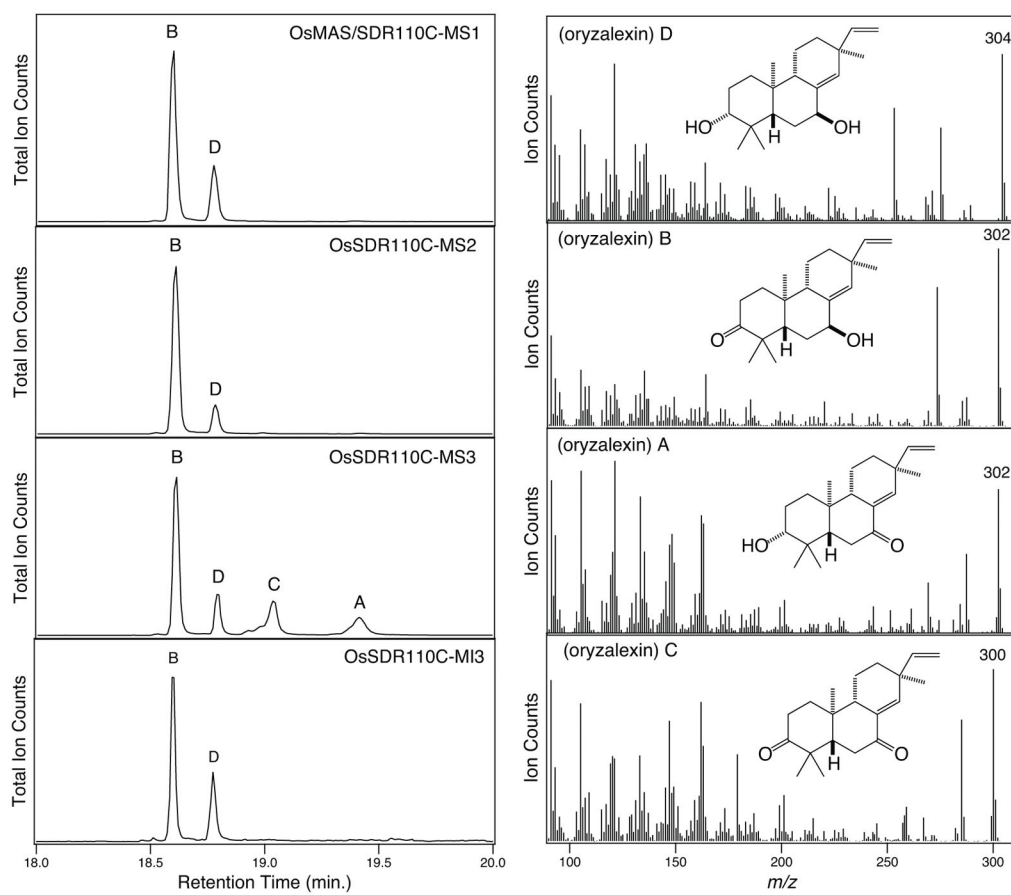
Figure 5.
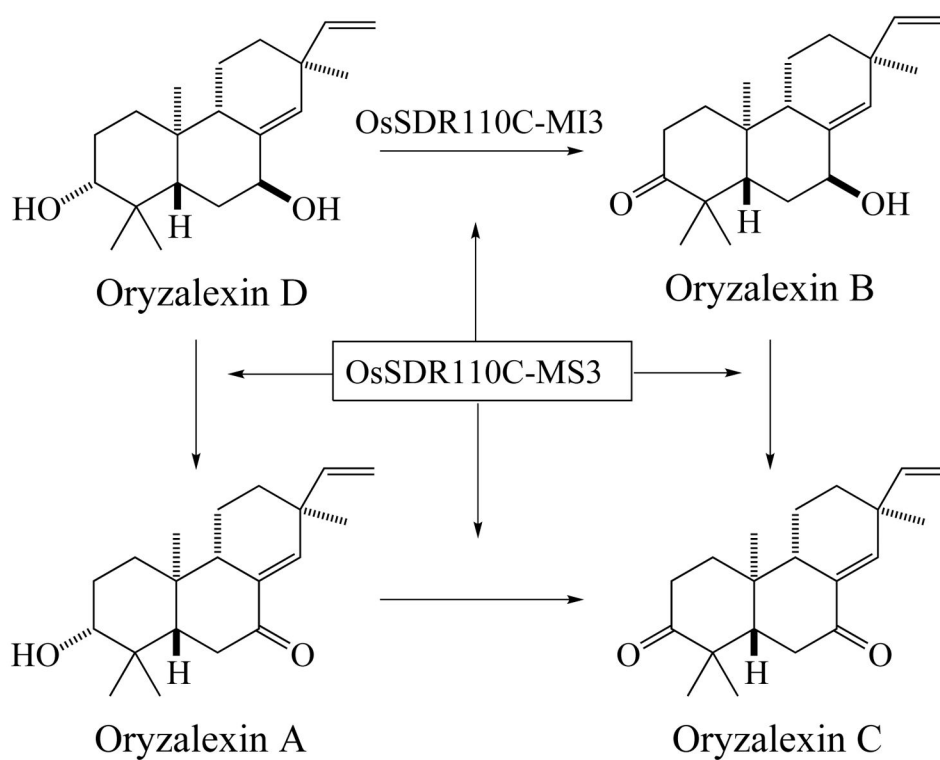GC-MS chromatograms and mass spectra demonstrating SDR activity with oryzalexin D.

Figure 6.
Biosynthesis of oryzalexins A – C from oryzalexin D by MI3 and MS3 indicated by the results reported here.

Table 1

OsSDR110C activity against oxygenated diterpenes.[a]

Substrate	MS1	MS2	MS3	MI2	MI3
3β-hydroxy-*syn*-pimaradien-19,6β-olide	+++	+++	++	–	+++
3β-hydroxy-*syn*-pimaradiene	+/–	+++	+	–	+++
oryzalexin D	+++	+++	+++	–	+++
3α-hydroxy-*ent*-sandaracopimaradiene	+/–	+	++	–	+++
7β-hydroxy-*ent*-sandaracopimaradiene	–	–	+	–	–
2α-hydroxy-*ent*-cassadiene	+++	+++	+++	–	+
3α-hydroxy-*ent*-cassadiene	++	++	+++	–	++
11α-hydroxy-*ent*-cassadiene	–	–	–	–	–

[a]Conversion rates: +++, > 50%; ++, 16–49%; +, 1–15%; +/–, <1%; –, not detectable.

Table 2

OsSDR110C kinetic parameters with biosynthetic intermediates.

Substrate	SDR110C-	K_M (μM)	k_{cat} (s^{-1})	k_{cat}/KM (s^{-1} M^{-1})
3β-hydroxy-*syn*-pimaradien-19,6β-olide	MS1	900 ± 400	$(8 ± 3)$ x10^{-2}	9 x10^1
	MS2	200 ± 100	$(4 ± 1)$ x10^{-1}	2 x10^3
oryzalexin D	MS1	60 ± 15	$(2 ± 1)$ x10^{-2}	3 x10^2
	MS2	60 ± 20	$(2.3 ± 0.3)$ x10^{-2}	4 x10^2
	MS3	40 ± 20	1.9 ± 0.2	5 x10^4
	MI3	14 ± 10	2.7 ± 0.4	2 x10^5